Available online at www.sciencedirect.com

SciVerse ScienceDirect

Ceramics International 38 (2012) 1577–1584

CERAMICS INTERNATIONAL

www.elsevier.com/locate/ceramint

Microwave-assisted solvothermal preparation and photoluminescence properties of Y_2O_3:Eu^{3+} phosphors

Fu-Wen Liu, Chia-Hao Hsu, Fu-Shan Chen, Chung-Hsin Lu *

Department of Chemical Engineering, National Taiwan University, Taipei, Taiwan, ROC

Received 10 February 2011; received in revised form 18 March 2011; accepted 10 April 2011
Available online 29 September 2011

Abstract

Europium doped yttrium oxide phosphors were synthesized by a rapid microwave-assisted solvothermal method. The microwave processing time for synthesizing the precursors of Y_2O_3:Eu^{3+} powders was as short as 5 min. After calcination at 600 °C, a well-crystallized pure phase of Y_2O_3:Eu^{3+} was obtained. The morphology of the precipitated powders was spherical and composed of nano-sized grains. As the microwave irradiation time was increased, the average particle size of the spherical powders increased, and the crystallinity of heat-treated powders was also enhanced. The synthesized powders retained the spherical morphology after heating treatments. An intense red emission at 611 nm was assigned to the $^5D_0$–$^7F_2$ transition of Eu^{3+}.

Keywords: D. Y_2O_3; Microwave; Solvothermal; Spherical; Methanol

1. Introduction

Field emission displays (FEDs) are considered to be one of the promising flat panel displays (FPDs) due to the superior properties, such as high brightness, high contrast, wide viewing angle, and fast response time [1–3]. For improving the performance of color purity in FEDs, developing phosphors with sufficient brightness and high chemical stability is required. Recently, oxide-based phosphors for FEDs have been intensively searched because of the good stability under high current density [4]. Among oxide-based phosphors, europium activated yttrium oxide (Y_2O_3:Eu^{3+}) is known as one of the promising phosphors, due to its short decay time, high luminescence, long-term thermal stability, and sharp red emission [5–7].

Y_2O_3:Eu^{3+} phosphors have been synthesized via different methods. In the solid-state method, the required temperature is higher than 1000 °C [8–10]. The high-temperature heating usually results in unfavorable coarsening of particles and serious aggregation. In the conventional solvothermal and hydrothermal processes, the processing temperature is reduced. However, the required heating time is relatively long (4–72 h) [5,11–14]. In order to overcome the drawbacks of these methods, it is necessary to develop a new process for synthesizing Y_2O_3:Eu^{3+} phosphors.

The microwave-hydrothermal method allows the formation of several oxides with controlled particle sizes and well-defined morphologies [15–18]. The microwave-hydrothermal process presents interesting advantages when compared to the conventional methods, such as (a) low synthesis temperatures, (b) short processing durations, and (c) formation of different morphologies [19].

A facile microwave-assisted solvothermal route has been used to synthesize ceramic powders, such as SnO_2, ZnO, ZrO_2, Sr_2CeO_4 and $Y_3Al_5O_{12}$, in a short processing time [20–23]. The advantages of the microwave process are attributed to the rotation of the dipolar molecules in the solution under the influence of an applied microwave electric field. During this process, molecules lose energy in the form of heat by molecular friction [22,24–26]. Thus, the heat is produced within the liquid and not transferred from the vessel as in the other conventional system [27]. Therefore, the microwave-assisted process can provide uniform heating and shorten the reaction time for synthesizing ceramic powders. In addition, the morphology and size of formed particles can be well controlled by changing solvents and reaction time [20,26,28]. Compared with conventional methods, the microwave-assisted process is found to be a convenient and

* Corresponding author. Tel.: +886 2 23651428; fax: +886 2 23623040.
E-mail address: chlu@ntu.edu.tw (C.-H. Lu).

0272-8842/$36.00
doi:10.1016/j.ceramint.2011.09.044

energy efficient route to produce ceramic powders [29,30]. In the present study, the microwave-assisted solvothermal process was utilized to synthesize spherical Y_2O_3:Eu^{3+} phosphors. The effects of microwave irradiation time on the structure and morphology of Y_2O_3:Eu^{3+} powders were investigated. The effects of calcination temperature on the photoluminescence properties of Y_2O_3:Eu^{3+} phosphors were also studied.

2. Experimental

Y_2O_3:Eu^{3+} powders were prepared via the rapid microwave-assisted solvothermal route. The molar ratio of Y^{3+}:Eu^{3+}:O^{2-} was set to 1.86:0.14:3. Stoichiometric oxides of each element were dissolved in HNO_3, and the mixed solution was stirred at room temperature for 3 h. Methanol was added with threefold volume of the above solution. The microwave-assisted solvothermal reaction was treated in a double walled vessel. The microwave system (MLS 1200 Mega) was operated at a frequency of 2.45 GHz and a fixed power of 500 W at 180 °C. The mixed solution was heated with microwave irradiation for 5, 10, 15 and 20 min. Under microwave irradiation, white precipitates were immediately formed. The formed precipitates were dried at 70 °C in an oven for 2 h. Microwave-derived precursors were further calcined in a regular box furnace at 600 °C for 2 h in air. In order to investigate the effects of calcination temperature on the microstructural and photoluminescence properties of Y_2O_3:Eu^{3+} powders, the precursor obtained after microwave irradiation for 15 min was further calcined at 800 °C, 1000 °C, 1200 °C and 1400 °C for 2 h in air.

The crystal structure of as-synthesized and calcined powders was investigated using an X-ray diffractometer (XRD, Philips X'Pert/MPD) operated at 45 kV and 40 mA. The morphology of powders was examined using a scanning electron microscope (SEM, Hitachi, S-800) and a transmission electron microscope (TEM, Hitachi H-7100). The photoluminescence properties of the prepared powders were analyzed using a fluorescence spectrometer (Hitachi, F-4500). A 150 W Xe lamp was used as a multi-wavelength light source. The equipped photomultiplier tube (PMT) (Hamamatsu R928) was operated at 400 V. The excitation spectra for samples were monitored by an emission wavelength at 611 nm, and the emission spectra were recorded by exciting the sample at 254 nm.

3. Results and discussion

3.1. Effects of microwave irradiation time on structure and morphology of Y_2O_3:Eu^{3+} powders

Fig. 1(a) illustrates the XRD patterns of the microwave-derived Y_2O_3:Eu^{3+} powders after microwave irradiation for 5 min. No characteristic diffraction peaks were observed, implying that the as-prepared powders were in an amorphous phase. Fig. 1(b)–(e) illustrates the XRD patterns of 600 °C-calcined powders obtained after microwave irradiation for 5, 10, 15 and 20 min, respectively. These XRD patterns exhibited well-resolved diffraction peaks, indicating that well-crystallized powders were formed. No impurity phases were detected

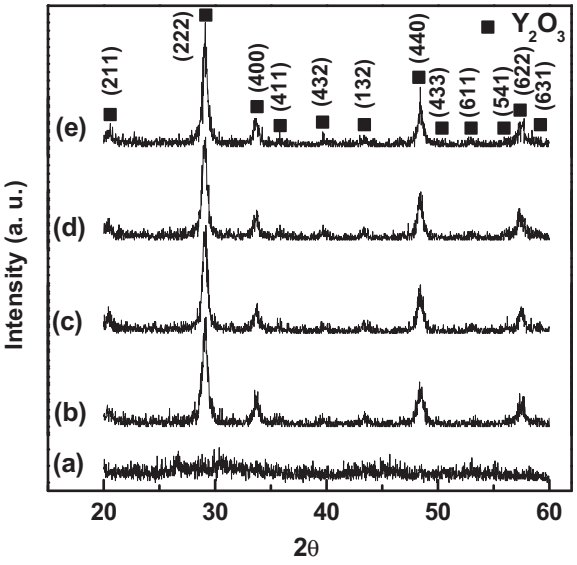

Fig. 1. X-ray diffraction patterns of as-prepared Y_2O_3:Eu^{3+} powders obtained under microwave irradiation for (a) 5 min, and 600 °C-calcined Y_2O_3:Eu^{3+} powders obtained under microwave irradiation for (b) 5 min, (c) 10 min, (d) 15 min and (e) 20 min.

in the diffraction patterns. The obtained diffraction patterns were consistent with the data reported in ICCD No. 89-5592 [31]. It was confirmed that the single cubic phase of Y_2O_3:Eu^{3+} powders was obtained. The reaction temperature for synthesizing single phase of Y_2O_3:Eu^{3+} powders is above 1000 °C in the solid state method [9,32]. However, in the microwave-assisted solvothermal process, the reaction temperature for synthesizing pure phase of Y_2O_3:Eu^{3+} powders is reduced to 600 °C. This is attributed to the improved compositional homogeneity and the enhanced reactivity in the microwave-derived precursors, thereby reducing the required heating temperature for preparing Y_2O_3:Eu^{3+} powders.

The crystallite sizes of the calcined powders were calculated from the FWHM (full width of half maximum) of the (2 2 2) diffraction peak in the XRD patterns using Scherrer's equation. The crystallite size of 600 °C-calcined Y_2O_3:Eu^{3+} powders obtained after microwave irradiation for 5 min was 18.7 nm. When the microwave irradiation time was increased to 20 min, the crystallite size of formed powders increased to 20.8 nm. It was found that the crystallite size of Y_2O_3:Eu^{3+} powders increased with an increase in the microwave irradiation time.

Fig. 2 shows the TEM micrograph and the selected area electron diffraction (SAED) pattern of the powders obtained by microwave irradiation for 5 min. The TEM micrograph shows that the as-prepared powders had a spherical shape with an average diameter of 1–2 μm and were softly agglomerated. Some nano-sized grains may be clearly observed on the surface of the spherical particles. The SAED pattern showed diffused halo rings, indicating the amorphous nature. When the microwave irradiation time was prolonged to 10, 15 and 20 min, the as-prepared powders SAED pattern did not change.

The SEM images of as-prepared powders obtained by under 5, 10, 15 and 20 min irradiation are shown in Fig. 3(a)–(d), respectively. In Fig. 3(a), the microwave-derived powders

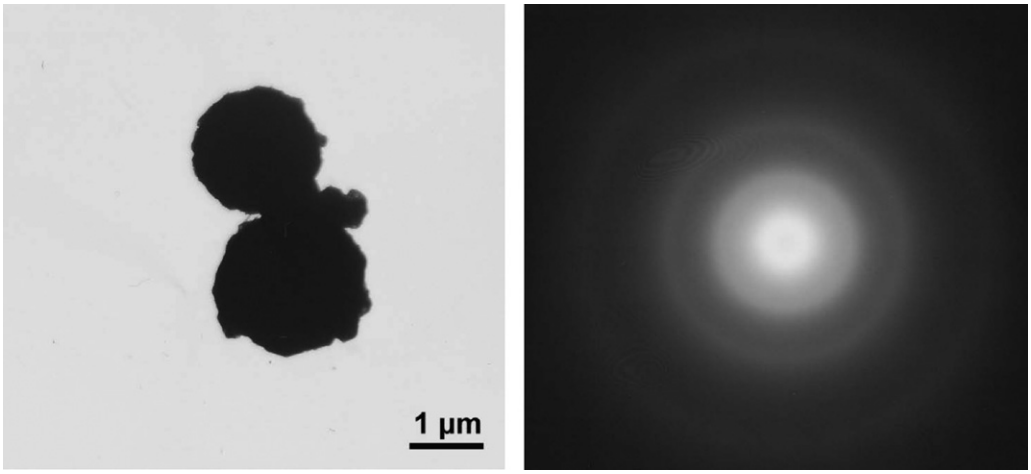

Fig. 2. Transmission electron micrograph and selected area electron diffraction pattern of as-prepared powders obtained under microwave irradiation for 5 min.

consist of spherical particles with an average size of around 1 μm. With an increase in the microwave irradiation time, the particles of the as-prepared powders became enlarged (as seen in Fig. 3(b)–(d)). The enlarged SEM photographs of as-prepared powders obtained under microwave irradiation for 5 and 20 min are shown in Fig. 3(e) and (f), respectively. Fig. 3(e) shows that Y_2O_3:Eu^{3+} microspheres consist of nano-sized grains with a size of 40–50 nm. The average particle size of nano-sized grains increases to around 70–80 nm as the microwave irradiation time increases to 20 min (Fig. 3(f)).

The pH value of the solution was measured in order to clarify the effects of the used solvent on the microstructure of the prepared powders. When CH_3OH was used as the solvent, the pH value of the solution before microwave irradiation was 0.37. After microwave irradiation for 5 min at 180 °C, the pH value of the resultant solution increased to 3.46, and white precipitates were formed immediately. As the microwave irradiation time was prolonged, the pH of the resultant solution did not vary. The change in pH before and after the microwave irradiation implies that hydroxyl groups formed during the reaction. In the alcoholic-based solution, the trivalent yttrium ions would form complexes with hydrophilic hydroxyl of alcoholic molecules. The complexes were protected by adsorbing hydrophobic hydrocarbyl of alcoholic molecules [20]. The absorbed layer of hydrophobic hydrocarbyl organic molecules on formed particles will constitute a steric barrier to prevent coagulation between particles [33]. Therefore, spherical Y_2O_3:Eu^{3+} particles can be formed.

3.2. Effects of microwave irradiation time on morphology and photoluminescence properties of calcined Y_2O_3:Eu^{3+} powders

Fig. 4(a)–(d) shows the morphology of 600 °C-calcined Y_2O_3:Eu^{3+} powders under microwave irradiation of 5, 10, 15 and 20 min, respectively. As seen in Fig. 4(a), the average particle size of 600 °C-calcined Y_2O_3:Eu^{3+} powders was around 1 μm. The average particle sizes of 600 °C-calcined powders shown in Fig. 4(b) and (c) were similar to those of powders shown in Fig. 3(b) and (c), respectively. In Fig. 4(d), the average particle size of 600 °C-calcined Y_2O_3:Eu^{3+} powders was 2 μm. It was observed that Y_2O_3:Eu^{3+} powders maintained the spherical morphology, and no significant grain growth occurred after calcination at 600 °C. In the sol–gel method, the prepared Y_2O_3:Eu^{3+} powders exhibit irregular shape and significantly aggregate [34–37]. The microwave-assisted solvothermal process is demonstrated to improve the morphology and dispersion state of Y_2O_3:Eu^{3+} phosphors.

Fig. 5 shows the TEM micrograph and SAED pattern of 600 °C-calcined Y_2O_3:Eu^{3+} phosphors under 5 min microwave irradiation. The average particle size of the spheres was around 1.5 μm. From SAED pattern of Y_2O_3:Eu^{3+} phosphors, the rings and dot patterns were clearly observed, indicating the polycrystalline nature of calcined powders. The rings resulted from the (2 1 1) and (2 2 2) planes for the cubic phase of Y_2O_3:Eu^{3+} powders. No significant change in the SAED pattern was observed when the microwave irradiation time was further prolonged.

The emission and excitation spectra of 600 °C-calcined Y_2O_3:Eu^{3+} phosphors obtained after various microwave irradiation times are illustrated in Fig. 6. The main peaks in the excitation spectra appeared in the range of 230–300 nm. They were attributed to the charge transfer between Eu^{3+} and O^{2-}. Several weak peaks were observed in the range of 350–500 nm. They were ascribed to the f–f transitions of Eu^{3+}. In the right part of Fig. 6, all peaks in the emission spectra corresponded to $^5D_0$ to ^7F_J transitions ($J = 0$, 1, 2 and 3) of Eu^{3+} in Y_2O_3:Eu^{3+} phosphors. The intense red emission at 611 nm was generated from the $^5D_0$–$^7F_2$ forced electric dipole transition [38]. The increase in photoluminescence intensity was ascribed to the improvement in the crystallinity and the grain growth of particles [9,39].

3.3. Effects of calcination temperatures on the photoluminescence properties of Y_2O_3:Eu^{3+} phosphors

Fig. 7 illustrates the XRD patterns of the microwave-derived powders calcined at various temperatures for 2 h, respectively.

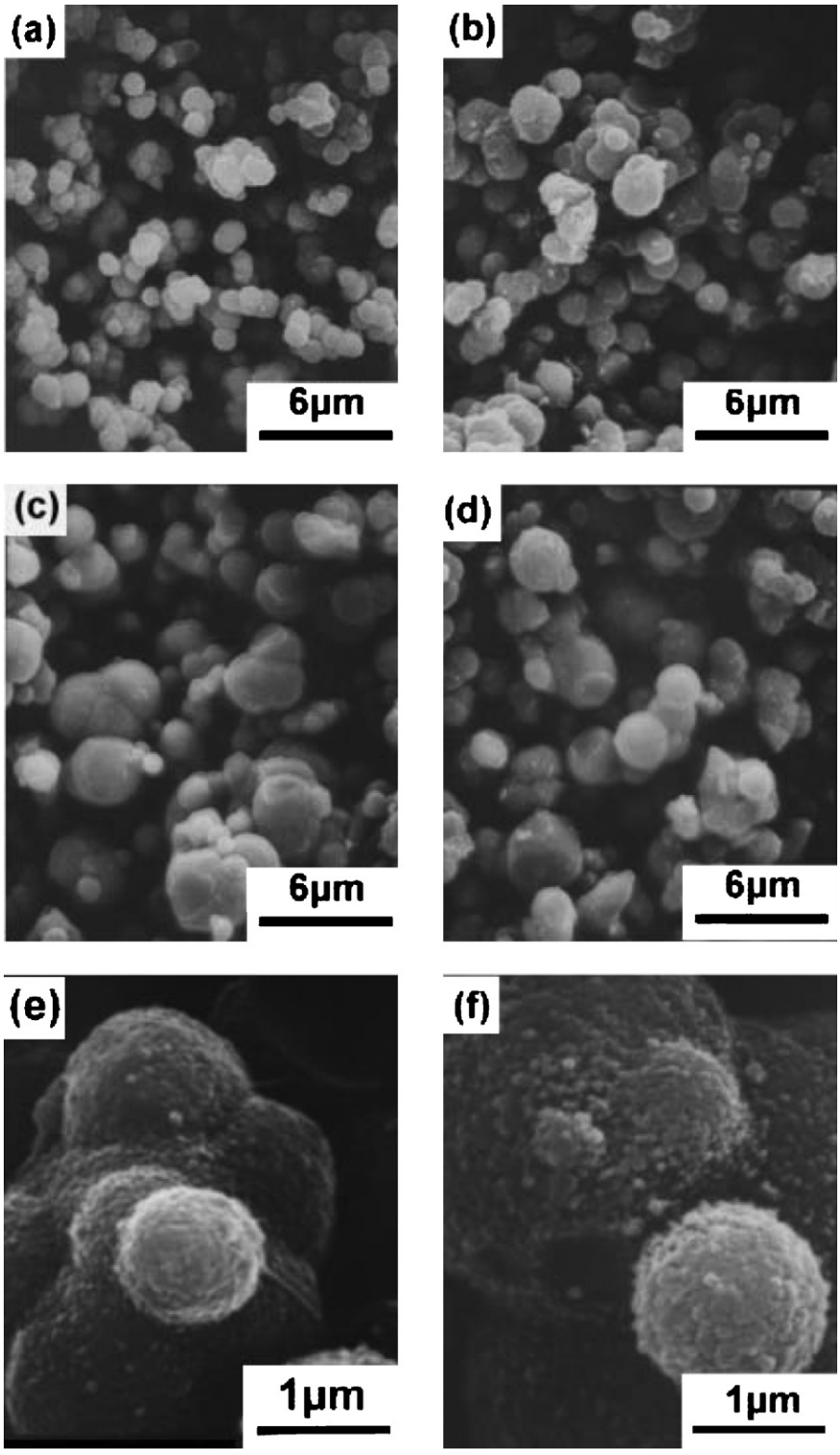

Fig. 3. Scanning electron micrographs of as-prepared Y_2O_3:Eu^{3+} powders obtained under microwave irradiation for (a) 5 min, (b) 10 min, (c) 15 min and (d) 20 min. The enlarged scanning electron micrographs of as-prepared Y_2O_3:Eu^{3+} powders obtained under microwave irradiation for (e) 5 min and (f) 20 min.

Increasing calcination temperature resulted in an increase in the intensity of diffraction peaks. The crystallite size of the calcined Y_2O_3:Eu^{3+} powders calculated from the XRD patterns using Scherrer's equation was 20.7 nm after calcinations of 600 °C. That increased to 69.2 nm after calcinations of 1400 °C with the crystallinity gradually increasing with a rise in calcination temperature.

Fig. 8(a)–(d) shows the SEM micrographs of the microwave-derived Y_2O_3:Eu^{3+} phosphors calcined at 800 °C, 1000 °C, 1200 °C, and 1400 °C for 2 h, respectively. In Fig. 8(a), the

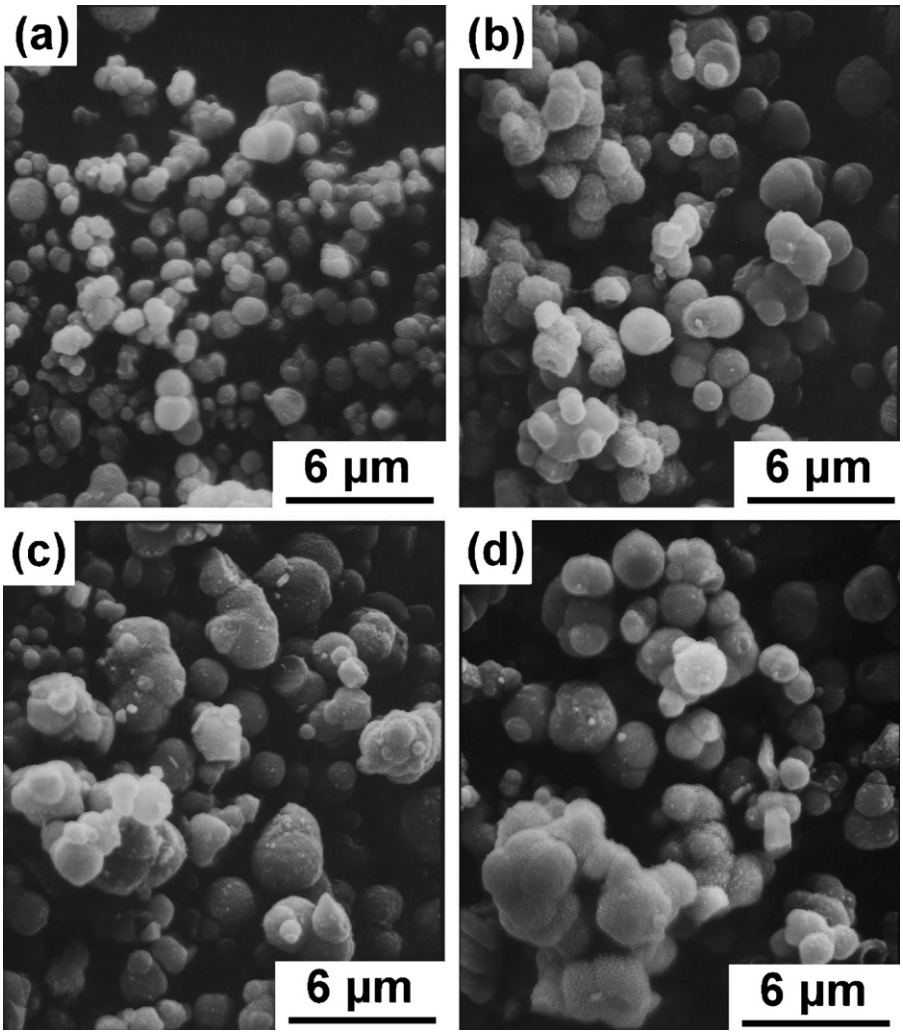

Fig. 4. Scanning electron micrographs of 600 °C-calcined Y_2O_3:Eu^{3+} powders prepared under microwave irradiation for (a) 5 min, (b) 10 min, (c) 15 min and (d) 20 min.

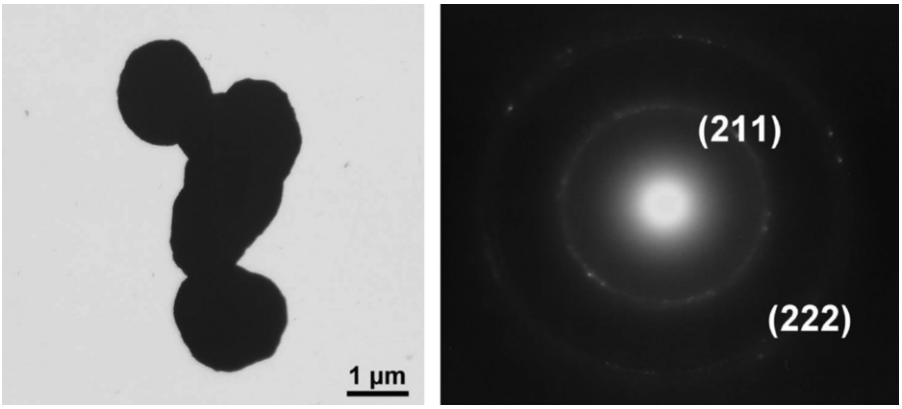

Fig. 5. Transmission electron micrograph and selected area electron diffraction pattern of 600 °C-calcined Y_2O_3:Eu^{3+} powders obtained under microwave irradiation for 5 min.

average particle size of 800 °C-calcined Y_2O_3:Eu^{3+} phosphors was around 2–3 μm. It is observed that Y_2O_3:Eu^{3+} phosphors remained the spherical shape as the calcination temperature increased. After calcination at 1400 °C, Y_2O_3:Eu^{3+} powders were softly agglomerated as shown in Fig. 8(d).

Fig. 9 illustrates the excitation and emission spectra of microwave-derived Y_2O_3:Eu^{3+} phosphors calcined at 600–1400 °C for 2 h. The 1400 °C-calcined Y_2O_3:Eu^{3+} phosphors exhibited the highest intensity of excitation and emission peaks. The photoluminescence intensity intensively increased with

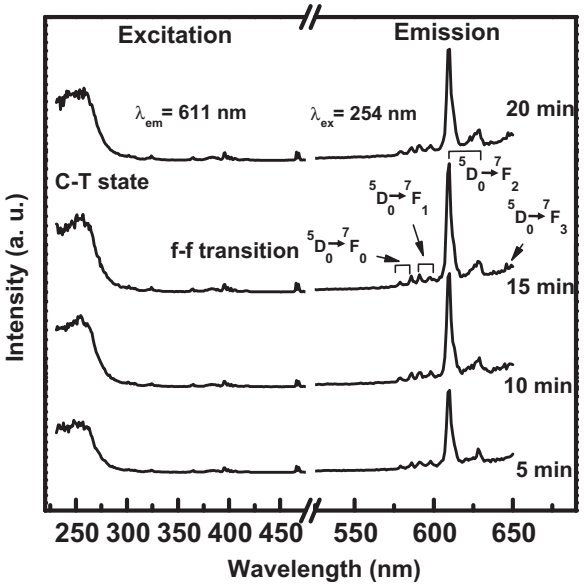

Fig. 6. Excitation ($\lambda_{em} = 611$ nm) and emission ($\lambda_{ex} = 254$ nm) spectra of 600 °C-calcined Y_2O_3:Eu^{3+} phosphors obtained via treating various microwave irradiation times.

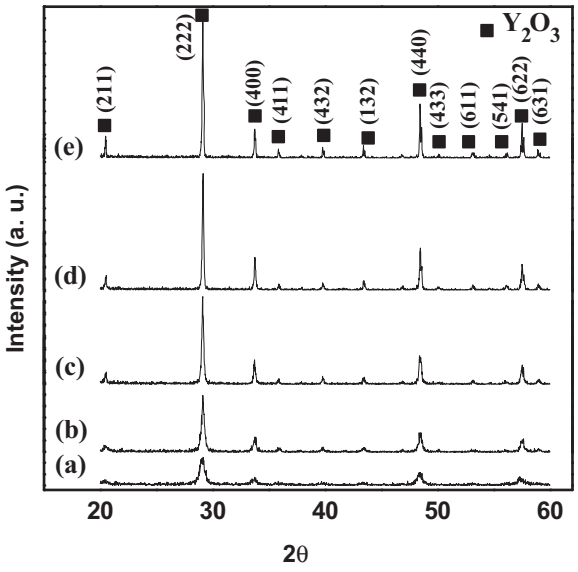

Fig. 7. X-ray diffraction patterns of the microwave-derived Y_2O_3:Eu^{3+} phosphors calcined at (a) 600 °C, (b) 800 °C, (c) 1000 °C, (d) 1200 °C and (e) 1400 °C for 2 h.

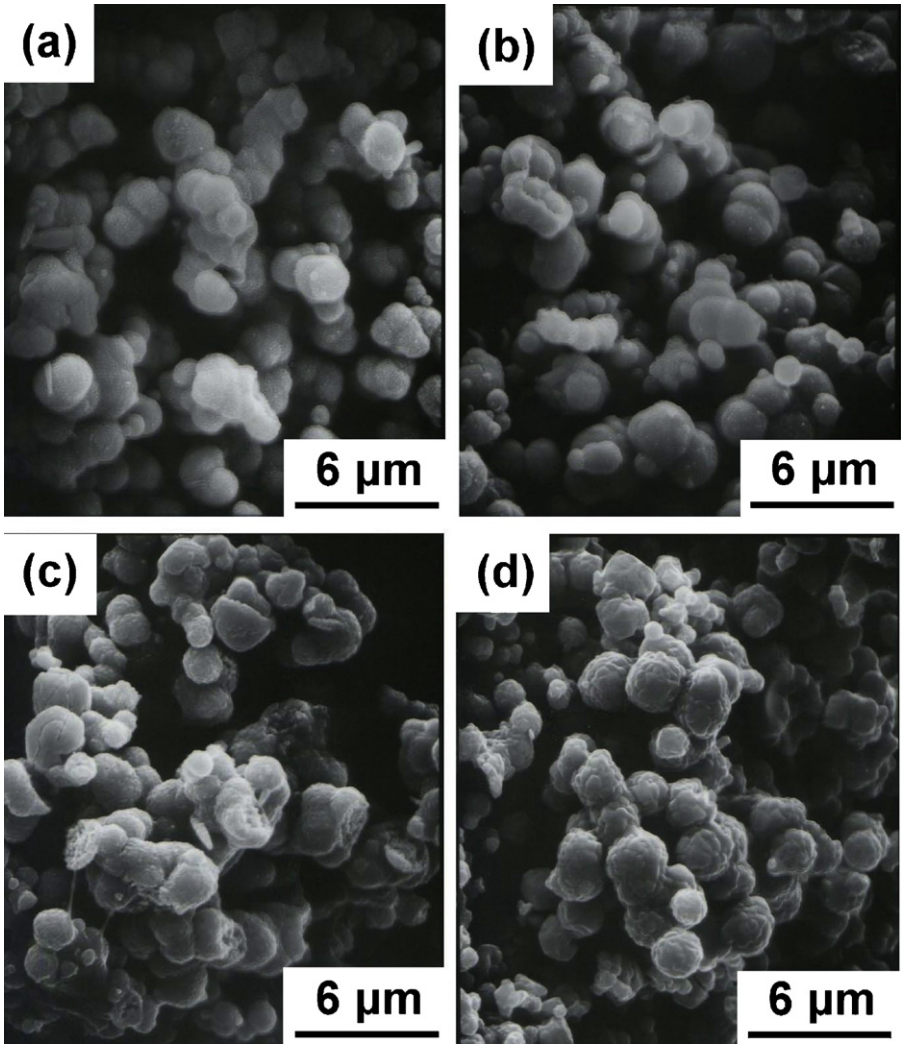

Fig. 8. Scanning electron micrographs of the microwave-derived Y_2O_3:Eu^{3+} phosphors calcined at (a) 800 °C, (b) 1000 °C, (c) 1200 °C and (d) 1400 °C for 2 h.

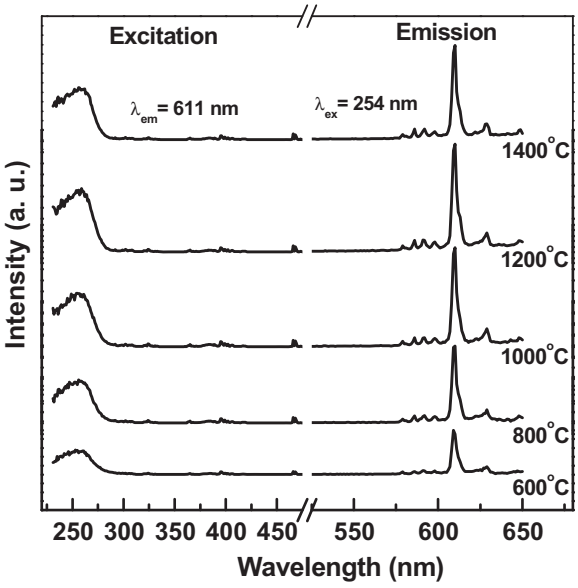

Fig. 9. Excitation (λ_{em} = 611 nm) and emission (λ_{ex} = 254 nm) spectra of the microwave-derived Y_2O_3:Eu^{3+} phosphors calcined at elevated temperatures.

increasing calcination temperatures because of the improvement in the crystallinity. Fig. 10(a) and (b) exhibits the variation of the photoluminescence intensity and crystallite size of the microwave-derived Y_2O_3:Eu^{3+} phosphors as a function of microwave irradiation time and of calcination temperature. The crystallite size and photoluminescence intensity raised with increasing the microwave irradiation time (Fig. 10(a)). Moreover, the crystallite size and photoluminescence intensity also increased with increasing calcination temperatures (Fig. 10(b)). The increase in emission and excitation intensity mainly derived from the enhanced crystallinity of Y_2O_3:Eu^{3+} phosphors.

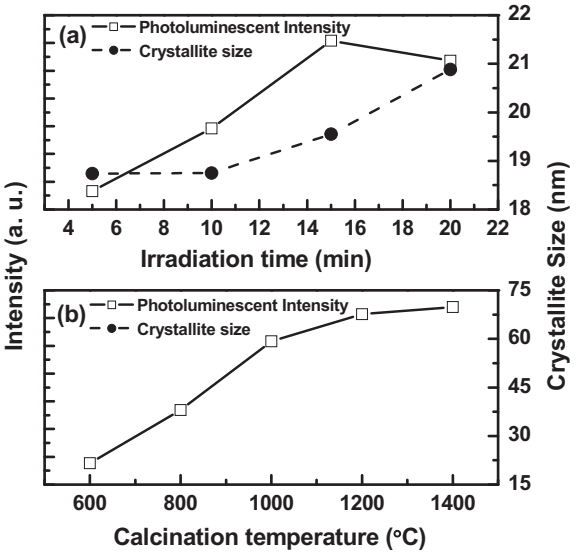

Fig. 10. Variation of photoluminescence intensity and crystallite size of the microwave-derived Y_2O_3:Eu^{3+} phosphors as a function of (a) microwave irradiation time and (b) calcination temperature.

4. Conclusions

A rapid microwave-assisted solvothermal route has been developed for synthesizing spherical Y_2O_3:Eu^{3+} phosphors. The microwave-assisted solvothermal processing time was as short as 5 min. The morphology of as-prepared powders was spherical. With an increase in microwave irradiation time, the particle size of the as-prepared powders increased. After calcination at 600 °C, cubic Y_2O_3:Eu^{3+} was formed. The red emission at 611 nm of Y_2O_3:Eu^{3+} phosphors was attributed to the $^5D_0$–$^7F_2$ transition of Eu^{3+}. When the microwave irradiation time was increased, the photoluminescence intensity of Y_2O_3:Eu^{3+} phosphors correspondingly increased.

References

[1] J.A. Nelson, E.L. Brant, M.J. Wanger, Nanocrystalline Y_2O_3:Eu phosphors prepared by alkalide reduction, Chem. Mater. 15 (2003) 688–691.
[2] S. Shionoya, W.M. Yen. (Eds.), Phosphor Handbook, CRC Press, Washington, DC, 1998.
[3] G. Blasse, B.C. Grabmaire (Eds.), Luminescence Materials, Springer, Berlin, 1994.
[4] P. Psuja, D. Hreniak, W. Strek, Low-voltage cathodoluminescence properties of $Y_3Al_5O_{12}$:Tb^{3+} nanopowders, J. Alloys Compd. 451 (2008) 571–574.
[5] J. Wan, Z. Wang, X. Chen, L. Mu, Y. Qian, Shape-tailored photoluminescent intensity of red phosphor Y_2O_3:Eu^{3+}, J. Cryst. Growth 284 (2005) 538–542.
[6] X. Hou, S. Zhou, Y. Li, W. Li, Luminescent properties of nano-sized Y_2O_3:Eu fabricated by co-precipitation method, J. Alloys Compd. 494 (2010) 382–385.
[7] S. Zhong, J. Chen, S. Wang, Q. Liu, Y. Wang, S. Wang, Y_2O_3:Eu^{3+} hexagonal microprisms: fast microwave synthesis and photoluminescence properties, J. Alloys Compd. 493 (2010) 322–325.
[8] W.C. Chien, Synthesis of Y_2O_3:Eu phosphors by bicontinuous cubic phase process, J. Cryst. Growth 290 (2006) 554–559.
[9] S.H. Shin, J.H. Kang, D.Y. Jeon, S.H. Choi, S.H. Lee, Y.C. You, D.S. Zang, Cathodoluminescence change of Y2O3:Eu phosphors by incorporation of Zn ions, Solid State Commun. 135 (2005) 30–33.
[10] M.V. Nazarov, J.H. Kang, D.Y. Jeon, E.J. Popovici, L. Muresan, B.S. Tsukerblat, Lattice parameter and luminescence properties of europium activated yttrium oxide, Solid State Commun. 133 (2005) 183–186.
[11] X. Bai, H. Song, G. Pan, Z. Liu, S. Lu, W. Di, X. Ren, Y. Lei, L. Fan, Luminescent enhancement in europium-doped yttria nanotubes coated with yttria, Appl. Phys. Lett. 88 (2006) 143104.
[12] A.V. Murugan, A.K. Viswanath, V. Ravi, B.A. Kakade, V. Saaminathan, Photoluminescence studies of Eu^{3+} doped Y_2O_3 nanophosphor prepared by microwave hydrothermal method, Appl. Phys. Lett. 89 (2006) 123120.
[13] R. Srinivasan, N.R. Yogamalar, J. Elanchezhiyan, R.J. Joseyphus, A.C. Bose, Structural and optical properties of europium doped yttrium oxide nanoparticles for phosphor applications, J. Alloys Compd. 496 (2010) 472–477.
[14] X. Bai, H. Song, L. Yu, L. Yang, Z. Liu, G. Pan, S. Lu, X. Ren, Y. Lei, L. Fan, Luminescent properties of pure cubic phase Y_2O_3/Eu^3+ nanotubes/nanowires prepared by a hydrothermal method, J. Phys. Chem. B 109 (2005) 15236–15242.
[15] S.A. Eliziário, L.S. Cavalcante, J.C. Sczancoski, P.S. Pizani, J.A. Varela, et al., Morphology and photoluminescence of HfO_2 obtained by microwave-hydrothermal, Nano. Res. Lett. 4 (2009) 1371–1379.
[16] L.S. Cavalcante, J.C. Sczancoski, J.W.M. Espinosa, J.A. Varela, P.S. Pizani, E. Longo, Photoluminescent behavior of $BaWO_4$ powders processed in microwave-hydrothermal, J. Alloys Compd. 474 (2009) 195–200.

[17] T. Thongtem, S. Kaowphong, S. Thongtem, Influence of cetyltrimethylammonium bromide on the morphology of AWO_4 (A = Ca, Sr) prepared by cyclic microwave irradiation, Appl. Surf. Sci. 254 (2008) 7765–7769.
[18] A. Phuruangrat, T. Thongtem, S. Thongtem, Preparation, characterization and photoluminescence of nanocrystalline calcium molybdate, J. Alloys Compd. 481 (2009) 568–572.
[19] L.S Cavalcante, J.C. Sczancoski, R.L. Tranquilin, J.A. Varela, E. Longo, M.O. Orlandi, Growth mechanism of octahedron-like $BaMoO_4$ microcrystals processed in microwave-hydrothermal: experimental observations and computational modeling, Particuology 7 (2009) 353–362.
[20] L. Xia, B. Yang, Z. Fu, Y. Yang, H. Yan, Y. Xu, S. Fu, G. Li, High-yield solvothermal synthesis of single-crystalline tin oxide tetragonal prism nanorods, Mater. Lett. 61 (2007) 1214–1217.
[21] Y.P. Fu, Preparation of $Y_3Al_5O_{12}$:Ce powders by microwave-induced combustion process and their luminescent properties, J. Alloys Compd. 414 (2006) 181–185.
[22] C.H. Lu, W.J. Hwang, S.V. Gobole, Microwave-hydrothermal synthesis and photoluminescence characteristics of zinc oxide powders, J. Mater. Res. 20 (2005) 464–471.
[23] C.T. Lee, F.S. Chen, C.H. Lu, Microwave-assisted solvothermal synthesis and characterization of SnO_2:Eu^{3+} phosphors, J. Alloys Compd. 490 (2010) 407–411.
[24] F. Bondioli, A.M. Ferrari, C. Leonelli, C. Siligardi, G.C. Pellancani, Microwave-hydrothermal synthesis of nanocrystalline zirconia powders, J. Am. Ceram. Soc. 84 (2001) 2728–2731.
[25] S. Komarneni, R. Roy, Q.H. Li, Microwave-hydrothermal synthesis of ceramic powders, Mater. Res. Bull. 27 (1992) 1393–1405.
[26] M. Tsuji, M. Hashimoto, Y. Nishizawa, M. Kubokawa, T. Tsuji, Microwave-assisted synthesis of metallic nanostructures in solution, Chem. Eur. J. 11 (2005) 440–452.
[27] A.V. Murugan, B.B. Kale, A. Kulkarni, L.B. Kunde, V. Saaminathan, Novel approach to control CdS morphology by simple microwave-solvothermal method, J. Mater. Sci. 16 (2005) 295–299.
[28] Z. Hua, X.M. Wang, P. Xiao, J. Shi, J. Eur. Ceram. Soc. 26 (2005) 2257.
[29] D. Keyson, D.P. Volanti, L.S. Cavalcante, A.Z. Simões, I.A. Souza, J.S. Vasconcelos, J.A. Varela, E. Longo, Domestic microwave oven adapted for fast heat treatment of $Ba_{0.5}Sr_{0.5}(Ti_{0.8}Sn_{0.2})O_3$ powders, J. Mater. Process. Technol. 189 (2007) 316–319.
[30] L.S. Cavalcante, V.S. Marques, J.C. Sczancoski, M.T. Escote, M.R. Joya, J.A. Varela, M.R.M.C. Santos, P.S. Pizani, E. Longo, Synthesis, structural refinement and optical behavior of $CaTiO_3$ powders: a comparative study of processing in different furnaces, Chem. Eng. J. 143 (2008) 299–307.
[31] X-ray Powder Data File, International Centre of Diffraction Data, Card. No. 89-5592.
[32] S.H. Shin, J.H. Kang, D.Y. Jeon, D.S. Zang, Enhancement of cathodoluminescence intensities of Y_2O_3:Eu and Gd_2O_3:Eu phosphors by incorporation of Li ions, J. Lumin. 114 (2005) 275–280.
[33] C. Jeffrey Brinker, W. George, Scherer (Eds.), Sol–Gel Science. The Physics and Chemistry of Sol–Gel Processing, Academic Press, Boston, 1990.
[34] V.B. Taxak, S.P. Khatkar, S.D. Han, R. Kumar, M. Kumar, Tartaric acid-assisted sol–gel synthesis of Y_2O_3:Eu^{3+} nanoparticles, J. Alloys Compd. 469 (2009) 224–226.
[35] J. Brubach, A. Dreizler, J. Janicka, Gas compositional and pressure effects on thermographic phosphor thermometry, Meas. Sci. Technol. 18 (2007) 764–770.
[36] A. Camenzind, R. Strobel, F. Krmeich, S.E. Pratsinis, Luminescence and crystallinity of flame-made Y_2O_3:Eu^{3+} nanoparticles, Adv. Powder Technol. 18 (2007) 5–8.
[37] C.H. Lu, H.C. Wang, Formation and microstructural variation of cerium carbonate hydroxide prepared by the hydrothermal process, Mater. Sci. Eng. B 90 (2002) 138–141.
[38] D.P. Volanti, I.L.V. Rosa, E.C. Paris, C.A. Paskocimas, P.S. Pizani, J.A. Varela, E. Longo, The role of the Eu^{3+} ions in structure and photoluminescence properties of $SrBi_2Nb_2O_9$ powders, Opt. Mater. 31 (2009) 995–999.
[39] C.H. Hsu, R. Jagannathan, C.H. Lu, Luminescent enhancement with tunable emission in Sr_2SiO_4:Eu^{2+} phosphors for white LEDs, Mater. Sci. Eng. B 167 (2010) 137–141.